Groundwater Project and eBooks:

An Envolving Platform for Groundwater Education and Practice

"Knowledge is power. Information is liberating. Education is the premise of progress, in every society, in every family."
- Kofi Annan, 1997

"Knowledge should be free and the best knowledge is free knowledge."
- Ying Fan Reinfelder, 2019

Edited by

John Cherry, G360 Institute for Groundwater Research, University of Guelph and
Distinguised Emeritus Professor, University of Waterloo, Canada

Gmail

Jaime Garfias <jgarfiass@gmail.com>

Your manuscript has been accepted

1 mensaje

Amanda Sills <amanda.sills@g360group.org> 10 de febrero de 2020, 9:03
Para: Jaime Garfias <jgarfiass@gmail.com>

Dear Dr. Garfias,

We are pleased to inform you that your chapter, "Case study: Prediction of sustainable management and associated land subsidence features in the Toluca aquifer system, Mexico", has been accepted for publication in the Ebook: An Evolving Platform for Groundwater Education and Practice. You will receive an-email in due course regarding the production process.

With best regards,

Amanda Sills, MSc, P.Geo.
Ebook Coordinator
G360 Institute for Groundwater Research
College of Engineering & Physical Sciences ¦ University of Guelph
50 Stone Rd E Guelph, ON, N1G 2W1
(519) 824-4120 ext. 53940 ¦ amanda.sills@g360group.org

Table 3: eBook Contributors Associated With 148 Organizations - September 13, 2019

Europe	North America	
Aarhus University	AECL	Shell Global Solutions
Beicip-Franlab	AECOM	Southwest Research Center
British Geologic Society	Air Force Institute of Technology	Stanford
Delft University of Technology	American Petroleum Institute	Syracuse University
ETH Zurich	ARCADIS	S.S.Papadopolous
Federal Inst. Geosci. & Ntrl Resources	Atomic Energy of Canada	Temple University
Geolog./ Geophysical Inst. of Hungary	Arizona State University	Tetratech
Geological Survey of Denmark and Greenland	Beatty and Associates Consulting	TRC Consulting
Karlsruhe Institute of Technology	BP	The University of New Mexico
University College London	Baker Law	The Water Institute U of Waterloo
Universite de Recherche INRS	Brown University	U.S. Geological Survey
University of Basilicata	Burns & McDonnell	UC Santa Cruz
University of Belgrade	Carleton University	Universite de Recherche INRS
University of Bologna	Chevron	University of Alberta
University of Lausanne	Colorado School of Mines	University of British Columbia
University of Leeds	Colorado State University	University of Buffalo
University of Liege	Columbia University	University of Calgary
University of Montpellier	Dalhousie University	University of California Davis
University of Oslo	Dickinson College	University of Guelph
University of Padova	Dillon Consulting	University of Houston
Sapienza University of Rome	Dordt University	University of Iowa
Sorbonne University	Environment Canada	University of Kansas
University of Strasbourg	EPA	University of Laval
University of Strathclyde	Exxon	University of Liege
Wageningen University	Geofirma Engineering Ltd.	University of Minnesota
World Health Organization	Geologic Survey of Canada	University of Montana
Asia	Georgia Tech	University of Nebraska
China University of Geosciences	Golder	University of New Brunswick
South China University of Sc. and Tech.	Geochimica	University of Nevada
University of Hong Kong	Haley Aldrich Consulting	University of Ottawa
South Africa	Hess Corp.	University of Quebec
Groundwater Africa	Hydrodynamics Group	University of Saskatchewan
Metago Water Geosciences	Integrated Sustainability Cnsltg	University of South Florida
Parsons and Assoc. Groundwater Consultants	King's College	University of Tennessee
Sinopec Research Institute	Mercer University	University of Texas
University of Free State	McGill University	University of Toronto
University of Pretoria	Michigan State University	University of Utah
University of Western Cape	NGWA	University of Washington
South and Central America	Natural Resources Canada	University of Waterloo
Autonomous University of the State of Mexico	New Mexico Tech	University of Quebec
Brazilian Geologic Survey	Orange County Water District	University of Wisconsin-Madison
City of Sao Paulo	Oregon State University	US Army Corps of Engineers
Federal University of Rio De Janeiro	Pacific Northwest Natl. Laboratory	USGS
Hidroplan Sustainable Water Institute	Princeton University	US Federal Institute Geoscience & Natural Resources
University of Sao Paulo	Partners in Hope	USGS Water Res. Mission Area
Vecttor	QED Environmental System	Vista Clara
Australia	Queen's University	Western University
Flinders University	Rutgers	Wilfrid Laurier University
CSIRO	Sacramento State University	World Bank

Domain Lead Kamini Singha

1. Overview: Role of geophysics in hydrogeologic problems: Kamini Singha, Frederick Day-Lewis
2. Electrical Resistivity: Frederick Day-Lewis, Kamini Singha, Tim Johnson
3. Induced Polarization:
4. Ground-penetrating Radar: Colby Steelman
5. Electromagnetic Induction: Anders Vest Christiansen
6. Self Potential: Damien Jougnot, Emily Voytek
7. NMR: Elliot Grunewald, Kristina Keating
8. Seismic: Jorden Hayes, Brady Flinchum
9. Fiber Optics: Scott Tyler, Nick van de Giesen, John Selker
10. Wireline Logging: John Williams
11. Airborne Methods: Burke Minsley
12. Tools for Fractured Rock
13. Rock Physics: Fred Nguyen
14. Joint Inversion: Erasmus Oware

38. IMPORTANT AQUIFER SYSTEMS AROUND THE WORLD

Chapters of the Domain:

1. High Plains Aquifer: USA
2. Edwards Aquifer: USA - Jack Sharp and Ron Green
3. Dakota Aquifer: USA
4. Milk River Aquifer: USA-Canada
5. California Central Valley Aquifer System: USA
6. Ogallala Aquifer: USA
7. Guarani Aquifer System: Brazil, Argentina, Paraguay, Uruguay - Roberto Kircheim
8. Permo-Triassic Aquifer: UK
9. the Chalk aquifer UK
10. Mexico Exemplary Example: Toluca Aquifer - Jaime Garfias
11. Mexico Valley Aquifer

39. COUNTRY BY COUNTRY OVERVIEWS OF HYDROGEOLOGY, GROUNDWATER USE AND PROBLEMS

40. DRILLING AND CORING METHODS

Chapters of the Domain:

1. Manual Well Drilling
2. Mechanized Well Drilling
3. Drilling Groundwater Monitoring Wells
4. Overburden Coring

41. STREAM, LAKE AND OCEAN MEASUREMENTS

Chapters of the Domain:

1. Stream Assessment and Gauging: Kamini Singha

Groundwater Project and eBooks: An Evolving Platform for Groundwater Education and Practice

Case study: Prediction of sustainable management and associated land subsidence features in the Toluca aquifer system, Mexico

Jaime Garfias[1], Richard Martel[2], Angus Calderhead[2], Pascal Castellazzi[3]

(1) Inter-American Institute of Technology and Water Sciences (IITCA). Autonomous University of the State of Mexico, Toluca, Mexico, C.P. 50130, Email: jgarfiass@gmail.com

(2) Institut National de la Recherche Scientifique (INRS-Été), Québec, QC G1K 9A9 Canada, Email: richard.martel@ete.inrs.ca, aicalderhead@gmail.com

(3) Commonwealth Science and Industrial Research Organisation (CSIRO), Land and Water Waite Rd, Urrbrae SA 5064, Australia. Email: Pascal.Castellazzi@csiro.au

Abstract

Regional land subsidence accompanying groundwater abstraction in the Toluca aquifer-system is a challenge for managing groundwater resources and mitigating associated hazards. In order to improve this situation, groundwater management scenarios for the Toluca Valley are examined with a three dimensional groundwater flow model coupled to a one dimensional compaction module. Subsequently, the land subsidence evolution was investigated by integrating SAR interferometry and geological and hydrogeological data to shed insight on the underlying processes governing subsidence. The results indicate that continuing at current rates of water consumption will lead to subsidence of more than 1.6 m over a 40 year period (2010–2050). Completely stopping exports to Mexico City is not the most important factor in controlling subsidence because the pumping system is mostly located in regions with low clay content, where subsidence is lower. However, decreasing exports by half and relocating the pumping centres to low-clay-content areas does have a positive effect on the overall water budget and subsidence. From 2003 to 2016, groundwater level declines of up to 1.6 m/yr, land subsidence up to 77 mm/yr, and major infrastructure damages are observed. Groundwater level data show highly variable seasonal responses according to their connectivity to recharge areas. However, the trend of groundwater levels consistently range from −0.5 to −1.5 m/yr regardless of the well location and depth. By analysing the horizontal gradients of vertical land subsidence, we provide a potential ground fracture map to assist in future urban development planning in the Toluca Valley. The approach taken in this study could be applied to their locations with similar problems in order to determine the most viable option for water supply.

Key words: Subsidence, aquifer exploitation, ground fracturing, horizontal gradient, InSAR, Toluca.

1 Introduction

Regional aquifer-system compaction is a natural or anthropogenic hazard that produces a downward displacement of the ground surface affecting large areas and important cities throughout the world (Galloway and Burbey, 2011; Calderhead et al., 2011). In many affected areas, increasing groundwater extraction is the only economically viable option. However, a direct consequence of heavy groundwater pumping in aquifers that are in hydraulic connection with thick compressible clays is the formation of fractures and land subsidence. The problems of groundwater depletion in response to groundwater abstractions include damage to housing and other civil infrastructures. The Toluca Valley has experienced such problems since the 1960's because of its geological setting and important groundwater pumping (Figueroa Vega, 1990; Figueroa Vega, 2004; Calderhead et al., 2011). The Toluca Valley's water resource and land subsidence problems are of interest because the basin was formally seen as an important source of water to the Mexico basin, yet today the Toluca Valley basin can no longer support its own growth let alone provide for another basin.

Several studies have focused on the hydrodynamics, hydrochemistry, groundwater depletion, and the related subsidence within the Toluca aquifer. Esteller and Andreu (2005) and Esteller et al. (2012) provided information on the changes in groundwater chemistry due to groundwater depletion. Rudolph et al. (2006) described the progressive hydrodynamic changes in the valley, which include the gradual extinction of lagoons, springs, and wetlands. Calderhead et al. (2011) provided an insight into groundwater dynamics and related aquifer-system compaction rates by integrating InSAR results and groundwater flow modeling to simulate future compaction rates (Calderhead et al., 2011, 2012a, 2012b). Similarly, Davila-Hernandez et al. (2014) used InSAR to compare hydraulic head losses in observation wells and land subsidence rates. Chaussard et al. (2014) and Castellazzi et al. (2016a) provided an overview of land subsidence problems in several cities of Central Mexico, including Toluca, by using time-series InSAR.

Alternatively, the use of numerical models to represent and predict subsidence (e.g. Gambolati, 1972; Helm, 1975; Leake and Galloway, 2007) has greatly enhanced the understanding and predictive capabilities of subsiding systems. It should be noted, however, that the theoretical assumptions and modeling approximations combined with a lack of representative geological, geomechanical, and hydraulic data can sometimes lead to numerical predictions that are not always reliable. Nonetheless, the application of consolidation theory to numerical models, constrained by field data and remote sensing techniques, remains the best approach for examining and predicting regional land subsidence (Galloway and Burbey, 2011; Calderhead et al., 2011; Gambolati and Teatini, 2019). Studies examining water resource management options (e.g., Rejani et al., 2008; Loukas et al., 2007; Sakiyan and Yazicigil, 2004) rarely consider land subsidence. Studies that have examined future subsidence (e.g., Rudolph and Frind, 1991; Ortega-Guerrero et al., 1999; Teatini et al., 2006) usually focus on groundwater pumping as the major factor influencing subsidence. Climate change (e.g., Larson et al., 2001), optimizing pumping locations (e.g., Bayer et al., 2009), and inter-basin water transfer are rarely considered. No studies have considered a combination of the above factors.

In view of the strategic importance of these resources in the region, and the conflicting evidence of potential impacts of excessive groundwater withdrawals and land subsidence, this study aims to establish a management policy for the sustainable development and management of the Toluca aquifer system for minimizing land subsidence. To that end it was envisaged to achieve the following objectives: i) to obtain a better understanding of the consequences of continued pumping of the Toluca Valley aquifer following existing trends; (ii) to determine the best scenarios for decreasing subsidence and maintaining a water supply to both the Toluca Valley and Mexico City and its metropolitan area and (iii) to investigate this evolution by integrating SAR interferometry and geological and hydrogeological data to evaluate the deformation features of hydrostratigraphic units. Given the increasing availability of archives from SAR satellites from all three generations of SAR satellites, it is now possible to follow subsidence rates over larger time-series and to

provide insight into the decadal-scale evolution of subsidence patterns. Such monitoring is particularly useful as the urban area and the transportation infrastructures are developing at alarming rates and as the groundwater crisis remains unsolved.

2. Description of the study area

2.1 Geographic Setting and Population Growth

The Toluca Valley is part of the Lerma-Santiago-Pacífico (LSP) water basin. It is located in the State of Mexico (Fig. 1) and extends over 2116 km^2. The basin is adjacent to the Mexico Valley, with the Sierra Las Cruces forming both a topographic and a hydraulic border between the two basins. The Lerma River originates in the lagoons of the south central part of the Toluca Valley; it is the second longest river in Mexico, emptying into Lake Chapala in the state of Jalisco. The Toluca Valley's proximity to Mexico City and rapidly developing infrastructure has allowed the city to grow into a major industrial zone for the country. The industrial corridor (Fig. 1) located to the East of downtown Toluca has a high concentration of industrial activity and is the area where most of the subsidence occurs.

According to the 2015 population estimates by region (CONAPO, 2015), the metropolitan area of Toluca, including 15 neighboring municipalities, is the fifth most populous metropolitan area in Mexico and the largest within the State of México. The total population of the Toluca Valley in 2015 was just over 2.2 million people (CONAPO, 2015). From 1960 to 2015, the population of the valley has doubled approximately every 20 years (INEGI, 1960; CONAPO, 2015). Fig. 2 shows a graphical comparison of the metropolitan urban area expansion in the Toluca Valley delimited using Landsat color-composite images from 1973 to 2015. As shown in this figure, the metropolitan urban area of the Toluca Valley expanded from 20.38 km^2 in 1973 to 478.57 km^2 in 2015 at an average rate of 10.9 km^2/yr. This expansion can be understood as natural urban growth due to economic and industrial development. The state of Mexico is an industrial centre with a range of economic activities; it is ranked second in the nation in terms of its GDP contribution, about 9.5 percent.

2.2 Geology and Hydrogeology

The Toluca Valley basin consists of two aquifer systems (Fig. 1); an alluvial aquifer in the upper portion and a fractured aquifer at the bottom (Lesser and Asociados, 1992; Ariel and Consultores, 1996). In the upper aquifer there are layers of clays that induce a local confinement. The Toluca Valley aquifer system is considered an unconfined aquifer because there is hydraulic connection between the alluvial aquifer and the fractured aquifer. Before the 1960's, groundwater levels in the Toluca Valley were either near surface or emerged above the land surface (Lesser and Asociados, 1992). Since the late 1960's, Mexico City and its metropolitan area began importing water on a large scale from other basins, including the Toluca Valley, to accommodate its water shortages. The Toluca Valley has continued to grow over the last four decades and presently, more than 935 pumping wells in the Toluca Valley are pumping over 469 Mm^3/yr (million cubic meters per year) (Calderhead et al., 2012b). Over one third of the total pumping comes from the Lerma system wells: a groundwater pumping system consisting of 230 pumping wells located along the upper section of the Lerma River. Most of the screens of the pumping wells cross both aquifer formations, therefore, water come from wells that draw from both aquifers. The system captures a large portion of the recharge water entering from the Sierra Las Cruces, and is then exported to the Mexico Valley and its metropolitan area at a rate of approximately 6.0 m^3/s (Rudolph et al., 2006; CONAGUA, 2007).

Regional groundwater flow, for the most part, is controlled by topography, where the primary recharge to the aquifers is in the mountains. Outcrops of fractured andesitic and basaltic rocks and pyroclastic material in the Nevado de Toluca and the Cruces mountains facilitate the direct

infiltration of precipitation to the aquifer, which then flows horizontally towards the centre of the valley (Eteisa, 1997; Grupo Herram, 1992). Groundwater flows preferentially in the aquifers through more permeable layers and channels in the fractured materials (Eteisa, 1995). Whereas historically, groundwater discharged in springs along the edges of the valley, and into the Lerma River system and the chain of lakes in the valley, extensive extraction from pumping wells throughout the valley have modified the historical groundwater flow patterns (Eteisa, 1995; Grupo Herram, 1992). Since the early 1950s, the regional groundwater flow field has been significantly affected by local groundwater extraction with the largest impacts associated with the Lerma system wells (Fig. 1), which has drawn flow towards the eastern flanks of the basin (CONAGUA, 2002; Eteisa, 1997). Based on measured hydraulic head conditions, the groundwater flow is now focused towards the Lerma system wells in the vicinity of the study site. Rudolph et al. (2006), Hancox et al, (2010), Calderhead et al. (2012b) provide additional background on analysis of the regional groundwater flow of the Toluca aquifer system.

3. Methodology

The research approach consists in presenting how the geologic model and mesh were constructed followed by a description of the various parameters chosen. The parameters discussed are: recharge with respect to climate change, pumping volumes for local use, export volumes to Mexico City and its metropolitan area, and relocating pumping wells within the valley. Finally, a combined analysis was applied to conduct a qualitative assessment by integrating SAR interferometry using 13 years of InSAR-derived ground displacement measurements.

3.1 Groundwater flow and subsidence simulation models

The HydroGeoSphere groundwater flow and transport model (Therrien et al., 2009) has been extended to improve the assessment and analysis of aquifer-system compaction. Within this framework, the integrated 3D-flow and 1-D instantaneous compaction finite-element numerical model was verified and applied to the Toluca aquifer system, Mexico (Calderhead et al., 2011). Simulations were constrained by remote sensing data (ranging from 2004 to 2008), extensometer readings (ranging from 2006 to 2008) and also hydraulic heads (measured quarterly since 1970) (Calderhead et al., 2010, 2011). Calderhead et al. (2011), Gallowey and Burkey (2011), Liu and Griffiths (2015) provide additional background on analysis and modeling of land subsidence accompanying deformation of aquifer systems. The simulated results from previous studies reproduced groundwater flow and aquifer-system compaction until the year 2009. In this approach, the study's model is based on the previous model; however, predictions are made using several scenarios until the year 2050.

In this context, a 3D geologic model domain (Fig. 3a) was created from 211 borehole logs and available cross sections. While preserving the general geologic topography, the generated 34 layers with 10 material types were simplified to 14 material layers with 6 material types. Thus, the topography of these geologic horizons was sequentially extracted at each node by 15 2D mesh layers. Using the GridBuilder software (McLaren, 2005), the final 2D mesh of 27225 nodes (Fig. 3b), representing the horizontal extent of the simulation domain, was generated with a mesh refinement around the location of 167 representative wells. The 3D mesh (Fig. 3d) was created by superposing the 15 2D mesh layers in the 3rd dimension (Fig. 3c). The 3D mesh has a total of 408375 nodes and 760284 elements. Table 1 presents a summary of the material properties for the simulated geologic layers. For additional details about the boundary conditions, initial conditions, pumping increments, and the solution method readers are referred to Calderhead (2009) and Calderhead et al. (2011).

For the purposes of this study, and to avoid excessive computation time, 167 representative wells were used with a relaxed mesh to simulate the more than the 935 pumping wells (Calderhead et al., 2011). In spite of all this, pumping rates are representative of the total pumping. Although higher pumping rates from fewer wells can locally lead to a misrepresentation of the drawdown and

subsidence, the regional extent of the drawdown and subsidence is generally representative of the observed behaviour (Calderhead et al., 2011).

3.2 Spatial distributed recharge

As emphasized by some researchers (Sophocleus, 2005), uncertainty and potential impacts of climate change on recharge are essential in determining the quantity and sustainability of a groundwater resource. Considering this fact, recharge was assumed to change as a function of climate change as outlined in the IPCC 2007 report (IPCC, 2007). Thus, historical data and climate change predictions for the area were input into the model from 1970 to 2050. Table 2 summarizes the variations of recharge used in the simulations. Spatially variable recharge was simulated using the HELP3 recharge model of the Toluca Valley (Calderhead et al., 2012b). Considering the increasing deficit within the basin, it was determined that over a long time (>10 years), seasonal head fluctuations did not have a significant impact on the total subsidence. Therefore, only yearly, as opposed to monthly or daily, recharge, discharge, and budget deficits were used for the simulations. For more details concerning the multiple parameters and source of data used in the HELP3 model, as well as recharge predictions for the Toluca Valley, the reader can refer to Calderhead et al. (2012b).

3.3 Groundwater pumping volumes

Groundwater pumping is one of the most difficult components to simulate groundwater flow because it has never been directly measured. For the present study, several assumptions have been made in creating this figure. Thus, to consider past pumping volumes of groundwater for local use, historical studies were used (OEE, 1970; Ariel and Consultores, 1996; CONAGUA, 2002; IMTA, 2003) and projections for future consumption were made using several assumptions. Projections of domestic use of groundwater are based on the population growth (INEGI, 2005). Over a 40 year period (2010–2050) projected annual population growth rates gradually decrease by 1.36 (1.34 to −0.2) for the average case (UNEP, 2008), 0.34 (1.34 to 1.0) for the worst case, and 1.64 (1.34 to −0.5) for the best case. Likewise, pumping for domestic use was assumed to increase proportionally to the population increases.

The State of Mexico presently contributes to 9.7% of Mexico's Gross Domestic Product (GDP) (INEGI, 2009). If it is assumed that this percentage remains constant in time and that the Toluca Valley's percentage of GDP remains constant in time, then Toluca's projected industrial use of water can also be based on Mexico's projected GDP (Hawksworth, 2006). Between 1989 and 1999, agriculture using irrigation fluctuated around 153 000 ha with no significant increase or decrease (INEGI, 2001); for lack of more information, it is assumed that agricultural use of water remains constant.

Prediction of environmental impacts of groundwater extraction requires detailed investigation of discharge processes. In this respect, export volumes to Mexico City have not increased in the last 10 years (Legorreta, 1997; CONAGUA, 2007), therefore a constant export volume (6.0 m^3/s) is assumed for the average projection. It is believed that legal action between the State of Mexico and Mexico City (Metropoli, 2008) will determine water exports from the Toluca Valley basin, and even decrease or stop altogether because the state of Mexico will be more protective of its water resources.

3.4 Location of pumping alternatives

The fraction of recharge that can theoretically be extracted from an aquifer under steady-state conditions will depend on the geometry of the aquifer system, and, in particular, on the location of the pumping wells relative to the natural recharge and discharge zones (Bredehoeft et al., 1982; Sphocleous, 2005). For this reason, Toluca and Mexico City and their metropolitan areas are now faced with building new pumping well networks to provide for the growing water demand. As was

done with the Toluca Valley over 40 years ago, adjacent basins are being drawn upon to provide for the more populated regions. The upper portion of the Balsas river basin (Sistema Cutzamala) and areas around Valle de Bravo are currently being used or are seen as good possibilities to provide for Mexico City and its metropolitan area and all municipalities located in the Toluca Valley (GEM, 2000).

In order for a groundwater system to be sustainable, pumping must be balanced by an equal capture of discharge and/or recharge. As an alternative, in order to improve this situation in the Toluca Valley, a series of scenarios with relocated wells is analyzed to evaluate the effects of existing and proposed pumping well networks on land subsidence. In that context, scenarios 1–3 (Table 3) examine worst case, best case, and average expected values based on Table 2. Recharge (based on Calderhead et al. (2010); and IPCC (2007)) and pumping are assigned their respective scenario based on Table 2 with pumping divided into (a) exports to the Mexico Valley and (b) local use. The pumping is divided into these two categories because local pumping is seen more as a function of a growing population whereas exports to the Mexico Valley are largely considered to be a political issue and legal battles could potentially lead to decreasing exports. Exports to the Mexico Valley are expected to increase (8 m^3/s) in the worst case scenario, decrease (3 m^3/s) in the best case scenario and remain constant (6 m^3/s) in the average expected scenario. A possible scenario is that pumping to the Mexico Valley decreases thus scenarios 4 and 5 decrease exports to 0 m^3/s and 3 m^3/s respectively while keeping average estimates for all other parameters. Scenario 6 examines the possibility of decreasing pumping in the Toluca Valley (−25%) and the Mexico Valley (−50%) to a more sustainable rate. Scenarios 7 and 8 make use of the clay thickness model (Fig. 4) for moving pumping wells from areas with high clay content to areas with lower clay content. Scenario 7 assumes average expected pumping and scenario 8 decreases pumping rates to scenario 6 values. By decreasing pumping for local use within the Toluca Valley, scenarios 6 and 8 imply inter-basin water transfer from surrounding basins.

Alternatively, other scenarios could have been considered such as including scenarios with efficient water use and expected artificial recharge, however it is estimated that these parameters are insignificant compared to values of groundwater pumping. For example, Calderhead et al. (2012b) estimates that a maximum artificial recharge would be in the order of 10 million cubic meters per year (Mm^3/year) for the entire Toluca Valley; this maximum value only represents less than 3% of the total recharge estimated at approximately 376 Mm^3/year.

3.5 Land subsidence detected by InSAR time series

3.5.1 Groundwater level monitoring and InSAR data

During this research, more than 10 water level data loggers (Solinst levellogger model 3001 or equivalent) were placed in monitoring wells in 2007, 2009 and 2012. The disaffected extraction wells in which pressure loggers were installed were chosen according to the recommendations of local water managers. In 2015, the loggers were retrieved and the recorded data were analyzed and entered into Matlab 2015a for analysis. No information on the stratigraphy of these observations wells is available. As the study focuses on the long term level variations, no barometric corrections are applied.

In order to estimate the aquifer-system compaction, 93 selected subsets of SAR images were used. They are all centered on the city of Toluca and cover from 7 to 15 km of distance in any direction from the city center. Based on these data, the SBAS-InSAR algorithm was applied over 33 Envisat ASAR IMS images, 19 Radarsat-2 Fine images, and 41 Sentinel-1A Interferometric Wide (IW) images covering different time periods (Castellazzi et al., 2017). For all InSAR processing, the topographic component of the phase variation signal was corrected using a Digital Elevation Model (DEM) with a 30 m resolution (ASTER GDEM Validation Team, 2009).

A comprehensive overview of the InSAR processing strategies used in this study and others is given by Crosetto et al. (2016). SAR data were processed using the Small BAseline Subset (SBAS-InSAR) algorithm (Berardino et al., 2002) and a Persistent Scatterers Interferometry (PSI) algorithm (Ferretti et al., 2001), both incorporated into the ENVI platform through the SARSCAPE 5.2 module (http://www.sarmap.ch/). SBAS is used for all three SAR time-series to produce combinable ground subsidence maps with the highest spatial coverage possible, thus highlighting the temporal evolution of subsidence patterns for the period 2003-2016. The PSI technique is only applied to the Sentinel-1A dataset to produce a gradient map at the highest resolution possible and for the most recent time-period. Its ability to precisely delineate ground fractures related to differential subsidence is tested. For more details concerning PSI and SBAS processing, as well as the methodology applied to produce interferograms using SAR images for the Toluca Valley, the reader can refer to Castellazzi et al. (2017).

3.5.2 Horizontal gradients and fracture delineation

As pointed out by Galloway and Burbey (2011), ground ruptures and fracturing can occur as a result of differential subsidence. They potentially causes important damage to urban infrastructures such as buildings, roads, pavement, communication and electricity lines, and water pipes, hence the need to monitor them. This phenomenon occurs mainly where subsidence patterns are spatially variable, as localized differential subsidence induces strain, bending of the surface layer, and ultimately result in tension cracks and fractures (Holzer and Johnson, 1985). In this study, horizontal gradients of vertical subsidence are analyzed in order to map areas prone to ground fracturing and thus provide operational support to urban planning. Castellazzi et al. (2017) provide additional background on the horizontal gradient calculation related to differential subsidence.

Taking into consideration the above results, a potential ground fracturing map was created by delineating manually the main features of the horizontal gradient map derived from the PSI vertical displacement map. In order to verify the occurrence of these potential fractures, a field validation survey was conducted in January 2017 and January 2019 to visit several easily accessible locations chosen throughout the study area. Signs of fractures and damages to infrastructures were checked at the vicinity of the delineated features. At several locations, local inhabitants greatly helped in identifying the effects of land subsidence. This field validation step is essential to assess the validity of the final PSI-derived potential ground fracturing map. The final map will be provided to the City of Toluca and to groundwater managers as guidance for urban development planning. It may also be provided to other cities of the region as an example.

4. Simulation of groundwater flow and regional land subsidence

In order to achieve a better understanding of the environmental impact of groundwater extraction, Fig. 5 presents the drawdown distribution for scenario 3 with pumping beginning in 1950 and results shown for years ranging between 1962 and 2050. The regional drawdown began around 1962 and increases over the years because of the increasing groundwater budget deficit. By 1990 there is already a marked drawdown of over 40 m in the centre of the valley. Hence, this progresses significantly over the following 60 years by increasing to over 120 m, in the industrial corridor, by 2050. The simulated groundwater level decline between 1970 and 2009 agrees quite well with observed field data (Calderhead et al., 2011).

Based on the simulations of the aquifer-system deformation, Fig. 6 shows the progression of total land subsidence occurrences in the Toluca Valley for different modeling scenarios. Results from 1962 to 2050 are based on the average expected scenario (scenario 3). Simulations begin in 1950 and only small occurrences of subsidence (<0.4 m) are observed in 1962. In that context, the occurrences are progressively larger from that point on and reach a maximum total subsidence of 3.8 m in 2050. Likewise, the area of maximum subsidence is located in the industrial corridor (Fig. 1) where high pumping rates, high drawdown, and thick compressible clay layers are observed.

According to previous studies (Figueroa Vega, 2004), even though pumping began before the 1960's it is estimated that regional land subsidence did not begin until heavy water exporting began in the late 1960's. In such a context, very few historical studies have examined regional land subsidence in the Toluca Valley, however, recent remote sensing techniques for measuring regional subsidence and field data were used to calibrate the model (Calderhead et al., 2010, 2011) giving more confidence in the 2010 case (Fig. 6d) and future scenarios. As mentioned before, within the content of this study, SAR interferometry was applied using 13 years of InSAR-derived ground displacement measurements.

In order to complete this section, Fig. 7 presents the resulting total compaction between 2010 and 2050 for the 8 scenarios. Note that this is cumulative compaction since 2010 and not since 1950 as presented in Fig. 6. Scenarios 1–3 demonstrate the effects of worst, best, and average case scenarios for the climate change and pumping parameters. Maximum total subsidence reaches 2.2 m for the worst case scenario (scenario 1), 1.4 m for the best case scenario (scenario 2), and 1.6 m for the average expected subsidence (scenario 3). Compared to other scenarios, the spatial extent of the affected area is similar and the differences in subsidence magnitude are within 0.8 m for the 40 year period.

As can be seen in Fig. 8, comparing scenarios 3, 4 and 5 is of interest for characterization land-surface motion in the Toluca Valley. There are only subtle differences between stopping exports (scenario 4) and cutting exports in half (scenario 5). However, there are noticeable differences between constant exports (scenario 3) and cutting exports in half (scenario 5).

It should be noted, however, that the most marked change in subsidence occurs when moving the pumping centres (scenarios 7 and 8) away from compressible clays. Total compaction can be drastically reduced by simply moving the pumping centres to different locations within the valley. The most desirable results (scenario 8) show a localized maximum subsidence of <0.3 m in 2050, otherwise there is only limited subsidence throughout the valley. Looking strictly at maximum vertical compaction (not regional extent) and comparing scenario 8 to the likely scenario 3, where pumping to the Mexico Valley remains constant and average expected pumping occurs (from 2010 to 2050), there is a maximum subsidence of over 1.6 m. In this context, in terms of maximum subsidence one can expect, vertically, 4 times more subsidence with scenario 8 compared to scenario 3.

5. Groundwater exploitation and subsidence conditions

It is possible that the theoretical assumptions and modeling approximations, combined with a lack of representative geological, geomechanical, and hydraulic data has led to unreliable numerical predictions. Nevertheless, the calibration process for the Toluca Valley flow and subsidence model (discussed more thoroughly in Calderhead et al., 2011), increases our confidence in the simulation results.

Under the conditions simulated, although the major factors controlling subsidence were varied in the simulations, for simplicity, some parameters that have an influence (e.g., geomechanical properties, extent of clay layers) were not varied. Likewise, there is also uncertainty in the chosen parameters. For instance the population growth is based on UN estimates for the country. Thus, an earthquake or a volcanic eruption in the valley would greatly throw off the population growth curve; hence the results should be viewed with caution.

As an alternative, climate change plays only a minor role in the occurrence of subsidence (Table 2). The three most important parameters controlling subsidence are local pumping volumes, relocating pumping wells within the valley, and export volumes to the Mexico Valley. It is apparent that continuing at the current rates of water consumption will lead to more subsidence. Even in the best

case scenario (scenario 2), maximum subsidence occurrences over a 40 year period (2010–2050) will reach 1.4 m.

Considering that the system pumping groundwater to the Mexico Valley is mostly located in regions with low clay content and little difference is observed between scenarios 4 and 5, completely stopping exports to the Mexico Valley (scenario 4) is not necessary for controlling the subsidence. Considering this fact, decreasing exports by half, decreasing domestic-use pumping, and relocating wells, does have a positive effect on the overall water budget and subsidence. It can be argued that all scenarios will require inter-basin water transfer at a later date because the water budget deficit is not sustainable.

Based on the above analysis, importing water from adjacent basins becomes necessary when decreasing pumping within the valley or there is an increase in the demand. In that context, inter-basin water transfer alone is not sufficient for controlling the subsidence. It is shown that a very effective way of controlling subsidence is by relocating the pumping centres to other locations with low clay content (scenarios 7 and 8). Hence, had pumping not occurred in the most compressible layers and a pumping system been in place to pump water to the urbanized part of the valley, much of the land subsidence could have been avoided. When planning water imports to the Toluca Valley from untapped basins, one could learn from the past and avoid drilling new wells in locations with thick compressible clay units, whether for exporting or local use.

In practice, however, it is probably not feasible to stop, or even decrease, pumping in the urbanized part of the Toluca Valley. In this schema, a costly infrastructure project would be required to import the water into the basin and supply the water to users in the urbanized part of the valley. Considering the likelihood of pumping continuing at current or greater rates, wells within the valley will probably be drilled to greater depths, further tapping the non-renewable resources and drawing on deeper, less potable water (Gárfias et al., 2008; Hancox et al., 2010).

As illustrated in this study, simulating scenarios with the numerical model is a viable tool when considering water management for limiting subsidence occurrences. The approach can be useful to other cities currently considering expanding their water supply and results can be used by resource managers and stakeholders for better management practices.

6. Characterization of the regional aquifer-system deformation

6.1 Groundwater depletion and land subsidence

As mentioned previously, a total of 93 SAR acquisitions from three orbital sensors were used to retrieve ground deformation data over 13 years: Envisat ASAR for 2003-2010, Rdarsat-2 for 2012-2014 and Sentinel-1A for 2014-2016. Based on these data, the accumulated compaction is as much as 1007 mm for the period of 2003-03-26 to 2016-04-12 (Fig. 8), corresponding to a mean rate of approximately 77 mm/yr. The highest subsidence rates are found on the western side of the urban area, along the industrial corridor located along the Toluca-Mexico highway, as have been observed previously within a preliminary study by Calderhead et al. (2011). Groundwater level vs subsidence time-series are shown in Figs. 9 and 10.

As illustrated in Fig. 6, wells 1, 2, 3, and 4 are located in highly subsiding areas. Seasonal variations of the water levels vary highly depending on the connections between the screened layer and the recharge zones. However, all of the four wells show negative level trends ranging from -1.12 to -0.28 m/yr. Well 2 and 3 are located in the industrial area, where important groundwater consumers are located. Water level from well 2 is notably influenced by a pumping well located nearby, and a highly varying groundwater level recovery and drawdown pattern is observed in relation to the pumping cycles of the extraction well. Important negative level trends can be observed in well 1, 2, and 4, while level variations in well 3 show an unexpected recovery from 2012, which could be potentially due to the decommissioning of a nearby pumping well. Well

4 is screened at the same depth as well 1, and both show similar level trends. However, a noticeable difference in the seasonal cycles suggests different hydraulic connections to their contributing recharge areas. Well 5 is located downgradient in the groundwater flow system, along the Toluca-Ixtlahuaca transportation axis, and away from the pumping centers. Even if only 2 years of data are available at this well, its shows both a seasonal signal and a strong negative level trend of −0.79 m/yr. This well, located on the lowest altitude of the Toluca valley, and along the groundwater discharge area of the Toluca Valley aquifer and away from all pumping centers provides information about the varying groundwater discharge rates, which are likely impacted by the groundwater extraction upstream.

As shown in Fig. 10, wells 6, 7, 8 and 9 are located outside of the InSAR subsidence survey. Well 6, 7 and 9 are located closer to the recharge area of the Sierra Las Cruces mountain range. Well 6 is strongly influenced by a pumping well drilled 20 m away, and it shows frequent sudden level variations as much as 8 m. The influencing pumping well is related to the Lerma system, providing water for exportation to the Mexico Valley. Well 7 and 8 do not show the typical ample temporal patterns expected near a recharge area and are probably poorly connected to it. However, they both show slightly negative trends reflecting the regional scale groundwater depletion occurring within the valley. On the contrary, well 9, located higher in the mountain range, shows very important amplitude and seasonal recharge patterns as much as 10 m typical for a well located in the Sierra Las Cruces, where the recharge rates are the highest of the valley.

6.2 Land subsidence rates and horizontal gradients

As described before, PSI processing was performed with 41 Sentinel-1A IW images to select and invert the phase variations into displacement for 567728 detected coherent ground targets spread over 750 km^2 (about 1/3 of the total Toluca basin area) and centered over the City of Toluca (Fig. 11). Vertical ground motion rates range from 0 to -80 mm/yr. The south-east and south-western sides of the urban area are facing generally increasing land subsidence rates. The latest measurements show that important land subsidence (superior to 50 mm/yr) is spreading to the east, along the Toluca-Mexico axis, and where important transportation infrastructure developments are planned to take place (Mexico News Daily, 2015). The subsidence is also spreading to the west, which now shows rates of subsidence up to 55 mm/yr. As a result, the industrial complex, several housing districts, and the airport are affected by important and spatially varying land subsidence patterns (Fig. 11a). The largest rates of subsidence are found in the lacustrine sediments (Figs. 1 and 11a), and the smallest rates occur where slightly coarser-grained alluvial sediments occur, or where alluvial sediment layers are thinner.

The methodology used to compute gradient allows delineating fractures without showing the typical artifacts related to interpolation in areas of low PS point density (Fig. 11b). Important gradient patterns occur within the valley, and their patterns differ significantly from the latest surficial mapping determined by the Ayuntamiento de Toluca (2013–Fig. 11b). As the work by the Ayuntamiento de Toluca (2013) is based on local knowledge and field observation, it might overlook the less noticeable fractures where population density is lower or where no complaints from local inhabitants were received. In addition, several fractures noticed in the field before 2004 do not show differential movements from 2014 to 2016, confirming the variable dynamics of compaction of the Toluca aquifer, with respect to variable temporal and spatial distributions of groundwater extraction and accompanying groundwater level drawdown and recovery. The most noticeable fractures (Figs. 11a and b) showed a differential displacement rate of around 30 mm/yr. Several subsidence horizontal gradient features show shapes aligned with mapped basaltic flows (Fig. 11b), which reflects the volcanic/alluvial history of the Toluca aquifer system controlling the sediment thickness and the subsidence patterns.

6.3 Field validation of the InSAR-derived ground fracturing map

We suggest that the ground fracture mapping is more complete and reliable when derived from InSAR than when solely based on field observations (Figueroa Vega, 2004; Ayuntamiento de Toluca, 2013). This hypothesis was tested through a field survey, which consisted in visiting several easily accessible potential fractures observed by InSAR (Fig. 12). Thus, as can be observed in Fig. 13, in some locations, obvious linear ground fractures are found (e.g. sites 1, 8, and 4), while in others, only discontinuous subsidence effects can be observed (e.g. sites 7 and 9). The latter can be interpreted as secondary effects of structural damage suggesting the possible occurrence of differential subsidence and ground ruptures.

Based on PSI processing, linear fractures were easily identified in the field at most locations (Sites 1, 2, 3, 4, 6, 8, 11, and 12 – Figs. 12 and 13). No obvious fractures were identified at the locations 5, 9, 10 and 7 (Fig. 12). The detection of important subsidence gradients does not directly imply that a fracture is observable. Three factors are likely to compromise the identification of fractures in the field. First, we suggest that infrastructures close to the city center (Sites 9 and 10) are better maintained and quickly repaired after been affected by differential subsidence. Second, the presence of high horizontal gradients of vertical subsidence does not necessarily imply observable ground fracturing. We suggest that where the strain is relieved progressively, in 'steps', it is divided over several smaller fractures, which compromises their identification. At these locations, damages to infrastructures might not be obvious enough to be observed while surveying, and might require a more in-depth and time-consuming field inspection. Third, the Gaussian filtering required to smooth out the noise (isolated unstable targets) and produce a usable gradient map leads to a decrease in resolution proportional to the Gaussian filter radius. It implies that fractures cannot be identified with a spatial precision sufficient for direct and effortless identification in the field. In most locations, the help of local inhabitants was essential to identify the fracture, which was not observable exactly in the field where it was drawn on the InSAR-derived map.

Taking into consideration the above results, and how there were also found ground fractures in 2/3 of the locations visited (e.g., Fig. 13), and given the difficulty of identifying such patterns in the field (i.e., some might have been missed), we conclude that the PSI-derived ground fractures map is generally reliable enough to provide guidance for urban development planning. Such a map can be used as is, i.e. as a potential ground fracturing map, but we recommend its use as an a priori map supporting a field-based ground fracture monitoring.

6.4Limitations and perspectives

The Toluca aquifer system is highly heterogeneous, and hydraulic connections between aquifers and recharge areas are not fully understood. Consequently, it is notably difficult to accurately estimate the regional scale groundwater depletion using only a few observation wells. However, given the drawdown rates observed in 9 wells monitored as part of this study, it is reasonable to estimate the regional groundwater level decline between 50 cm/yr to 80 cm/yr. This groundwater depletion leads to a land subsidence rate as much as 77 mm/yr during 2003–2016 and recurrent damages to infrastructures in both the eastern and western parts of the city. The city center, located on a thinner sediment layer deposited on an andesitic volcanic cone, does not face land subsidence issues. It is also one of the main geological structures controlling distribution and thickness of the compressible sediment and associated fracturing.

The latest surficial fracture map was published in 2013 (Ayuntamiento de Toluca, 2013), and shows different patterns than the ones revealed by the InSAR analysis in this study. Fractures are regularly monitored neither by the scientific community nor by local governments, suggesting that related prevention or mitigation programs in place are insufficient. In the meantime, major infrastructure developments are planned to better link Toluca and Mexico, suggesting the acceleration of the expansion and densification of the city of Toluca. Nevertheless, the groundwater depletion issues remain unresolved.

Sentinel-1 IW data are particularly suitable for the application presented in this article. PSI processing can provide high-resolution ground displacement maps over urban areas, but is also more sensitive than SBAS to inversion errors when displacement rates are important or non-linear. The 12 day orbital repeat path frequency (or 6 days when using both Sentienl-1 satellites) greatly helps in solving the phase ambiguity during the PSI phase/time to displacement/time inversion. In addition, the temporal density of the Sentinel-1 system allows performing PSI-derived fault detection analysis such as presented in this article over much shorter periods of time (i.e. the last 4–6 months). Such analysis is of great interest for cities, as fractures would be detected at their most early stage and as field validation would potentially be easier, without a time gap allowing residents to repair or hide the fractures.

Theoretically, 30 C-Band images per year (corresponding to a 12 days repeat path frequency) can reveal up to 42 cm/yr of subsidence without unwrapping error and using a typical PSI-type processing (Crossetto et al., 2016). As compacting aquifer-systems produce subsidence rates usually ranging from a few mm/yr to around 30 cm/yr, Sentinel-1 SAR data are perfectly suitable for such application. The use of both Sentinel-1 satellites, simulating a 6 day repeat path frequency, is useful to double the threshold of maximum measurable displacement, and most of all to better remove the atmospheric phase shifts and obtain a better vertical precision and detection threshold. It also opens perspectives for studying fractured rock aquifers (Schuite et al., 2015) or the least compressible sedimentary aquifers.

The low 3D perpendicular baseline (usually within the 20–100 m range for any given image pair) and the high orbital precision also greatly help in providing clean interferograms without important residual fringe patterns. Given the availability of the Sentinel-1 IW data and the maturity of both InSAR algorithms and processing platforms, InSAR-derived ground fracturing maps can be routinely provided to cities built over compacting aquifers in the near future. This will allow water-planners, hydrologists, police makers, and others stakeholders to develop water management plans, and make informed decisions based on the most recent and comprehensive data.

Acknowledgements. We are thankful to the Ministère des Relations Internationales du Québec, INRS-ETE, NSERC (a discovery grant held by Richard Martel), the Autonomous University of the State of México (UAEM), CONACyT, COMECyT, AUCC/IDRC, and the Ministère de l'Éducation du Québec for their financial support. The authors would also like to acknowledge the Natural Resources Canada (NRCAN) and the Canadian Space Agency (CSA) for their help in obtaining Radarsat-2 acquisitions over Mexico under the MURF #CG0063. The authors are also grateful to the European Space Agency (ESA) for providing Envisat ASAR images under project C1F.31647 and Sentinel-1 IW data. We also thank the French Center for Space Research (CNES) for proving a user-friendly access to Sentinel-1 data through the Plateforme d'Exploitation des Produits Sentinel (PEPS – https://peps.cnes.fr).

References

Ariel and Consultores, 1996. Estudio de Simulación Hidrodinámica y Diseño Optimo de las Redes de Observación de los acuíferos de Calera, San Luis Potosí y Toluca (Tomo 3: Acuífero de Toluca), Comisión Nacional del Agua, México, DF, 308 p.

ASTER GDEM Validation Team, 2009. ASTER global DEM validation summary report. METI & NASA 28 p.

Ayuntamiento de Toluca, 2013. Riesgos Geológicos en el Municipio de Toluca. H. Ayuntamiento de Toluca, 2013-2015. Plan Municipal de desarrollo urbano de Toluca. 550 p.

Bayer P, Duran E, Baumann R, Finkel M, 2009. Optimized groundwater drawdown in a subsiding urban mining area. J Hydrol 365(1–2):95–104.

Berardino P, Fornaro G, Lanari R, Sansosti E, 2002. A new algorithm for surface deformation monitoring based on small baseline differential SAR interferograms. IEEE Trans. Geosci. Remote Sens. 40, 2375–2383. http://dx.doi.org/10.1109/tgrs. 2002.803792. Biot, M., 1941. General theory of three-dimensional consolidation. J. Appl. Phys. 12 (2), 155–164.

Bredehoeft JD, Papadopulos SS, Cooper HH Jr, 1982. The Water Budget Myth. In: Scientific basis of water resource management, studies in geophysics. National Academy Press, Washington, DC, pp 51–57.

Calderhead AI, 2009. Pumping effects on land subsidence: assessment using field data, remote sensing and numerical modeling. PhD thesis. Institut national de la recherche scientifique, Université du Québec, 314 p.

Calderhead A, Martel R, Alasset P-J, Rivera A and Gárfias J, 2010. Land subsidence induced by groundwater pumping, monitored by D-InSAR and field data in the Toluca Valley, Mexico. Canadian Journal of Remote Sensing (Best paper Award 2010), vol. 36, No. 1, pp. 9-23.

Calderhead A, Therrien R, Rivera A, Martel R and Gárfias J, 2011. Simulating pumping-induced regional land subsidence in a complex aquifer system. Advances in Water Resources, Vol. 34(1), pp. 83-97.

Calderhead A, Martel R, Gárfias J, Rivera A and Therrien R, 2012a. Sustainable Management for Minimizing Land Subsidence of an Over-Pumped Volcanic Aquifer System: Tools for Policy Design. Water Resources Management, (ISSN: 0920-4741), vol. 26, No. 7, pp. 1847-1864

Calderhead A, Martel R, Gárfias J, Rivera A and Therrien R, 2012b. Pumping dry: an increasing groundwater budget deficit induced by urbanization, industrialization, and climate change in an over-exploited volcanic aquifer. Environmental Earth Sciences Journal, vol. 66, No. 7, pp. 1753-1767.

Castellazzi, P., Arroyo-Domínguez, N., Martel, R., Calderhead, A.I., Normand, J.C.L., Gárfias, J., Rivera, A., 2016a. Land subsidence in major cities of Central Mexico: interpreting InSAR-derived land subsidence mapping wit hydrogeological data. Int. J. Appl. Earth Obs. Geoinf. 47, 102–111.

Castellazzi, P., Garfias J, Martel R, Brouard C, Rivera A. 2017. InSAR to support sustainable urbanization over compacting aquifers: The case of Toluca Valley, Mexico. Int. J. Appl. Earth Obs. Geoinf. 65, 33-44.

Chaussard E, Wdowinski S, Cabral-Cano E, Amelung F, 2014. Land subsidence in central Mexico detected by ALOS InSAR time-series. Remote Sens. Environ, 140, 94–106.

Crosetto, M., Monserrat, O., Cuevas-González, M., Devanthéry, N., Crippa, B., 2016. Persistent scatterer interferometry: a review. ISPRS J. Photogramm. Remote Sens. 115, 78–89.

Davila-Hernandez, N., Madrigal, D., Exposito, J.L., Antonio, X., 2014. Multi-temporal analysis of land subsidence in Toluca valley (Mexico) through a combination of persistent scatterer interferometry (PSI) and historical piezometric data. Adv. Remote Sens. 3, 49.

CONAGUA, 2002. Determinación de la Disponibilidad de Agua en el Acuífero Valle de Toluca, Estado de México. Comisión Nacional del Agua, México, DF. 31 p.

CONAGUA, 2007. Comisión Nacional del Agua, Base de datos de los acuíferos a nivel Nacional y Regional. Comisión Nacional del Agua, Subdirección Nacional Técnica, Gerencia en el estado de México, 115 p.

CONAPO, 2015. Delimitación de las zonas Metropolitanas de México 2015. Consejo Nacional de Población, 286 p.

Esteller MV, Andreu JM, 2005. Anthropic effects on hydrochemical characteristics of the Valle de Toluca aquifer (central Mexico). Hydrol. J. 13, 378–390.

Esteller MV, Rodriguez R, Cardona A, Padilla-Sanchez L, 2012. Evaluation of hydrochemical changes due to intensive aquifer exploitation: case studies from Mexico. Environ. Monit. Assess. 184, 5725–5741.

ETEISA 1995. Estudio Para la Medición y Configuración Piezométrica de la Red de Pozos Piloto de la DGCOH en el Alto Lerma y Actualización y Digitalización del Plano Base de la Zona del Alto Lerma. Gobierno del Distrito Federal, Secretaria de Obras y Servicios (DGCOH), Contrato: 5-111-1-0182.

ETEISA, 1997. Estudio de Evolución de Niveles Piezométricos en la Cuenca del Alto Lerma Para el Periodo 1985-1997: Informe Final. Gobierno del Distrito Federal, Secretaria de Obras y Servicios (DGCOH), Contrato: 7-CO4-1-0371.

Ferretti A, Prati C, and Rocca F, 2001. "Permanent Scatterers in SAR Interferometry." IEEE Transactions on Geoscience and Remote Sensing 39 (1): 8–20. doi:10.1109/36.898661.

Figueroa Vega GE, 2004. El agrietamiento de la ciudad de Toluca. Consejo consultivo de Agua, December, 85 p.

Figueroa Vega GE, 1990. Estudio sobre el comportamiento reciente del acuífero de la ciudad de Toluca y su relación con el problema de agrietamientos de la zona poniente de la misma, CEAS, Estado de México, 235 p.

Galloway D, Burbey TJ, 2011. Review: Regional land subsidence accompanying groundwater extraction. Hydrogeol J 19:1459–1486.

Gambolati G, 1972. A three-dimensional model to compute land subsidence. Bullet Int Ass Hydrol Sci, 17:219–26.

Gambolati G, Teatini P, 2019. Groundwater and land subsidence. An Evolving Platform for Groundwater Education and Practice. In Ebook, An Evolving Platform for Groundwater Education and Practice. Edited by John Cherry, Institute for Groundwater Research, University of Guelph.

Gárfias J, Llanos H, Bibiano L, 2008. Uso Racional y Sostenible de los recursos hídricos del acuífero del valle de Toluca. Revista Ciencia Ergo Sum, Vol. 15–1, May–June 2008, pp. 61–72.

GEM, 2000. Horizontes del Agua en el Estado de México. Secretaría de Desarrollo Urbano y Obras Públicas, Comisión del Estado de México (Water Horizons in the State of Mexico. Ministry of Urban Development and Public Works Commission of the State of Mexico), 160 p

Grupo Herram, 1992. Estudio Hidrogeológico Regional de Toluca e Ixtlahuaca, Tomo I: Informe. DCGOH, Contrato No: 3-33-1-0162.

Hancox J, Gárfias J, Aravena R and Rudolph DL, 2010. Assessing the Vulnerability of over-exploited volcanic aquifer systems using Multiparameter Analysis, Toluca Basin, Mexico. Environmental Earth Sciences; Vol. 59(8), p. 1643-1660.

Hawksworth J, 2006. The World in 2050: how big will the emerging market economies get and how can the OECD compete? Pricewaterhouse Coopers, London.

Helm DC, 1975. One-dimensional simulation of aquifer system compaction near Pixley, California, 1, Constant parameters. Water Resour Res, 11:465–78.

Holzer TL, Johnson AI, 1985. Land subsidence caused by ground water withdrawal in urban areas. GeoJournal 11, 245–255.

Mexico News Daily, 2015. The Train That Budget Cuts Have Not Stopped. Mexico News Daily. Saturday, 21 March 2015.

IMTA, 2003. Censo del utilización del agua en el valle de Toluca. Instituto Mexicano de Tecnologia del Agua, 247 p.

INEGI, 1960. Censo general de población y vivienda, Instituto Nacional de Estadística,Geografía e Informática, 245 p.

INEGI, 2001. Síntesis de información Geográfica del Estado de México. Instituto Nacional de Estadística, Geografía e Informática.

INEGI, 2005. Censo general de población y vivienda 2005. Instituto Nacional de Estadística, Geografía e Informática.

INEGI, 2009. Síntesis de información Geográfica del Estado de Mexico/Aportación al Producto Interno Bruto (PIB) nacional. Instituto Nacional de Estadística, Geografía e Informática, http://cuentame.inegi.org.mx.

IPCC, 2007. Climate Change 2007: The Physical Science Basis. Contribution of Working Group I to the Fourth Assessment Report of the Intergovernmental Panel on Climate Change [Solomon, S., D. Qin, M. Manning (eds.)]

Larson KJ, Basagaoglu H, Marino MA, 2001. Prediction of optimal safe ground water yield and land subsidence in the Los Banos-Kettleman City area, California, using a calibrated numerical simulation model. J Hydrol 242(1–2):79–102.

Leake SA, Galloway DL, 2007. MODFLOW ground-water model—User guide to the Subsidence and Aquifer-System Compaction Package (SUB-WT) for watertable aquifers: US. Geological Survey, Techniques and Methods 6-A23, 42 p.

Legorreta J, 1997. Rainfall, the key to the future of the Valley of Mexico. La Jornada Ecologica 5(58):1–12

Lesser and Asociados, 1992. Estudio para el Diagnostico del acuífero del Valle de Toluca, para implementar la reglamentación de la extracción del agua subterránea, 325 p.

Liu, JC and DV, Griffiths DV, 2015. A general solution for 1D consolidation induced by depth- and time-dependent changes in stress, Géotechnique, 10.1680/geot.14.P.077, **65**, 1, (66-72).

Loukas A, Mylopoulos N, Vasiliades L, 2007. A modeling system for the evaluation of water. Resources management strategies in Thessaly, Greece. Water Resour Manage 21:1673–1702

McLaren RG, 2005. User Guide: GRID BUILDER A pre-processor for 2-D, triangular element,finite-element programs, University of Waterloo - Groundwater Simulations Group.

Metropoli, 2008. Pierde Edomex batalla legal sobre acuíferos. In: Metropoli (Editor). Metropoli, Mexico, Mexico, last accessed Nov, 2011. http://ciudadanosenred.com.mx/node/3399

OEE, 1970. Los acuíferos del alto Lerma pub. No. 7, (The upper Lerma Aquifers pub. No. 7). report for Oficina de estudios especiales (OEE) of the CHCVM-SRH

Ortega-Guerrero A, Rudolph D, Cherry J, 1999. Analysis of long-term land subsidence near Mexico City: field investigations and predictive modeling. Water Resour Res 35(11):3327–3341.

Rejani RM, Jha K, Panda SN, Mull R, 2008. Simulation modeling for efficient groundwater management in Balasore Coastal Basin, India. Water Resour Manage 22:23–50.

Rudolph DL, Frind EO, 1991. Hydraulic response of highly compressible aquitards during consolidation. Water Resour Res, 27(1):17–28.

Rudolph DL, Sultan R, Garfias J, McLaren RG, 2006. Significance of Enhanced Infiltration due to Groundwater Extraction on the Disappearance of a Large Wetland System: Lerma River Basin, Mexico. Hydrogeology Journal, vol. 14 (1-2), pp. 115-130.

Sakiyan J, Yazicigil H, 2004. Sustainable development and management of an aquifer system in western Turkey. Hydrogeol J 12:66–80.

Schuite J, Longuevergne L, Bour O, Boudin F, Durand S, Lavenant N, 2015. Inferring field-scale properties of a fractured aquifer from ground surface deformation during a well test. Geophys. Res. Lett. 42, 10696–10703. http://dx.doi.org/10. 1002/2015GL066387.

Sophocleous MA, 2005. Groundwater recharge and sustainability in the High Plains aquifer in Kansas, USA. Hydrogeol. J. 13:351–365.

Teatini P, Ferronato M, Gambolati G, Gonella M, 2006. Groundwater pumping and land subsidence in the Emilia-Romagna coastland, Italy: modeling the past occurrence and the future trend. Water Resour Res 42:W01406. doi:10.1029/2005WR004242.

Therrien R, McLaren G, Sudicky EA, Panday SM, 2009. User guide: hydrogeosphere – a three-dimensional numerical model describing fully-integrated subsurface and surface flow and solute transport, 430 p.

UNEP, 2008. Mexico's Annual population Growth Rate. United Nations Environment Programme data, http://www.unep.org/

Table 1. Description of calibrated material properties for the Toluca aquifer system obtained using the HGS model. Note that vertical hydraulic conductivity is assumed to be equal to horizontal hydraulic conductivity (modified from Calderhead et al. (2011)).

Layer number (From top to bottom)	Description	AT*	HC*	SS*	P*	F*	ES*	IS*
		b [m]	K [m/s]	S_s [1/m]	θ [-]	γ* [-]	S'_{ske} [1/m]	S'_{skv} [1/m]
Layer 1	clays 1	45.9	2.0E-06	5.6E-06	0.40	0.7	9.2E-07	3.7E-06
Layer 2	sand and gravel	18.0	4.0E-04	1.2E-06	0.35	1.0E-04	3.6E-08	1.4E-07
Layer 3	fine grains	16.9	3.0E-05	1.4E-06	0.30	1.0E-04	8.4E-08	3.4E-07
Layer 4	clay 2	2.1	2.0E-06	1.7E-06	0.35	0.7	3.0E-07	4.2E-07
Layer 5	fine grains	17.1	6.0E-05	1.4E-06	0.35	1.0E-04	8.6E-08	3.4E-07
Layer 6	coarse grains	19.0	1.0E-03	1.2E-06	0.35	1.0E-04	3.3E-08	1.3E-07
Layer 7	sand and gravel	10.6	4.0E-04	1.1E-06	0.35	1.0E-04	2.1E-08	8.5E-08
Layer 8	volcanic solids	6.7	6.0E-04	1.0E-06	0.30	1.0E-04	1.7E-12	6.7E-12
Layer 9	clays 3	21.9	5.0E-07	5.6E-06	0.35	0.7	2.1E-07	4.4E-06
Layer 10	conglomerate	7.3	6.0E-05	1.0E-06	0.30	1.0E-04	1.8E-12	7.3E-12
Layer 11	sand and gravel	6.8	4.0E-04	1.1E-06	0.35	1.0E-04	1.4E-08	5.4E-08
Layer 12	clays 4	3.7	6.0E-06	1.9E-06	0.35	0.7	1.9E-07	7.5E-07
Layer 13	fine grains	9.8	6.0E-05	1.2E-06	0.35	1.0E-04	4.9E-08	2.0E-07
Layer 14	sand and gravel	2.0	4.0E-04	1.0E-06	0.35	1.0E-04	4.0E-09	1.6E-08

* AT: Average thickness, HC: Hydraulic Conductivity, SS: Specific Storage, P: Porosity, F: Fraction of compressible materials, ES: Elastic skeletal specific storage, IS: Inelastic skeletal specific storage.

Tabla 2. Summary of the observed and expected groundwater recharge and pumping from 1970 to 2050. Total pumping is divided into domestic use and exports to Mexico City. Dates and scenarios with relocated wells are also indicated (modified from Calderhead et al. (2012a)).

		1970	1985	2000	2010	2020	2030	2040	2050
Recharge (Mm^3/yr)									
Historical		385.0	373.9	376.2	-	-	-	-	-
Averege		-	-	376.2	373.0	370.0	367.0	364.0	361.0
Wors case		-	-	376.2	358.4	340.8	323.2	305.6	288.0
Best case		-	-	376.2	377.8	379.6	381.4	383.2	385.0
Pumping (Mm^3/yr)									
Domestic use	Historical	-157.6	-212.2	-266.8	-	-	-	-	-
	Average	-	-	-	-305.3	-345.6	-382.6	-409.9	-428.7
	Worst case	-	-	-	-248.0	-294.8	-344.8	-398.4	-456.9
	Best case	-	-	-	-396.1	-426.4	-448.9	-461.5	-463.1
Export to Mexico City	Historical	-189.2	-189.2	-189.2					
	Average	-	-	-	-189.2	-189.2	-189.2	-189.2	-189.2
	Worst case	-	-	-	-252.3	-252.3	-252.3	-252.3	-252.3
	Best case	-	-	-	-94.6	-94.6	-94.6	-94.6	-94.6
Relocation of wells									
	Scenarios (1-6)	current	current	current	current	current	current	current	current
	Scenarios (7-8)	current	current	current	moved	moved	moved	moved	moved

Note: see Figure 5 for location of moved wells and Table 3 for description of pumping scenarios. '-' implies data is not relevant.

Table 3. Summary of pumping scenarios simulated with HGS between 2010 and 2050 to estimate land subsidence in the Toluca aquifer system (after Calderhead et al. (2012a).

Scenario	Lerma pumping (to Mexico City)	Toluca pumping	Recharge	Description
1	33% increase	worst case	worst case	Worst case expected with 33% increased Lerma pumping
2	50% decrease	best case	best case	Best case expected with 50% decrease in Lerma pumping
3	constant at 6 m^3/s	average	average	Average case with Lerma pumping constant at 6 m3/s
4	stop Lerma pumping (0 m^3/s)	average	average	Average case with stopping Lerma pumping
5	50% decrease	average	average	Average case with a 50% decrease in Lerma pumping
6	50% decrease	decrease by 25%	average	Decrease Lerma pumping by 50% and decrease Toluca Basin pumping by 25%
7	Constant at 6 m^3/s	average	average	Move pumping centres to locations with less clay (see Fig. 4)
8	50% decrease	decrease by 25%	average	Move pumping centres to locations with less clay (see Fig. 4) and decrease Toluca Basin pumping by 25% and Lerma Pumping by 50%

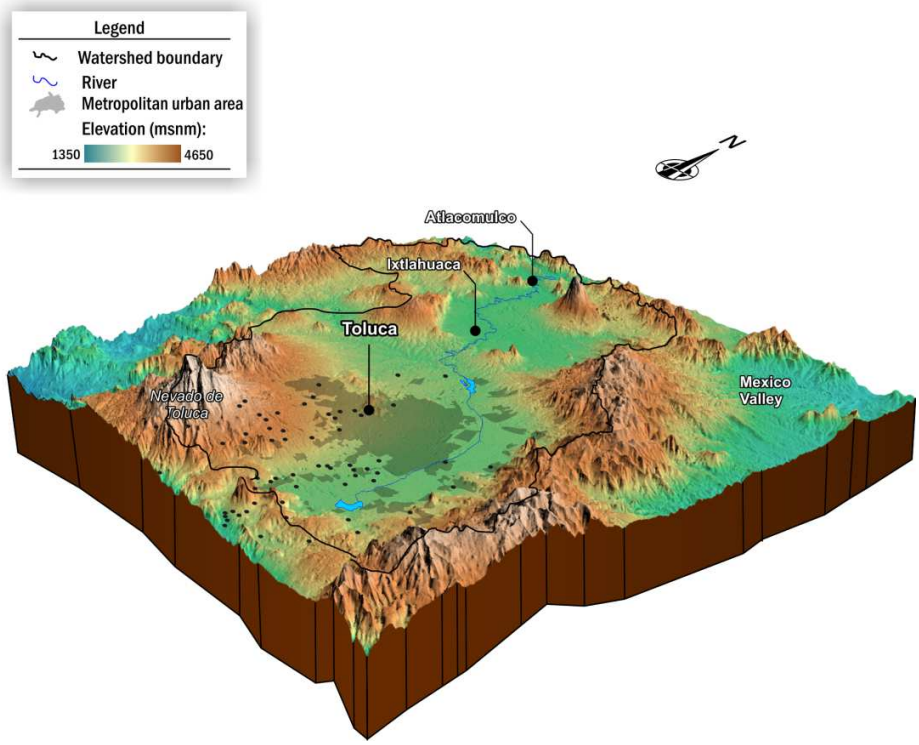

Figure 1. Three-dimensional schematic model of the Upper Lerma River Basin showing principal physiographic features and the extent of the Atlacomulco/Ixtlahuaca basin to the north and the Toluca basin to the south. Also shown is the metropolitan area for 2015 delimited using Landsat images.

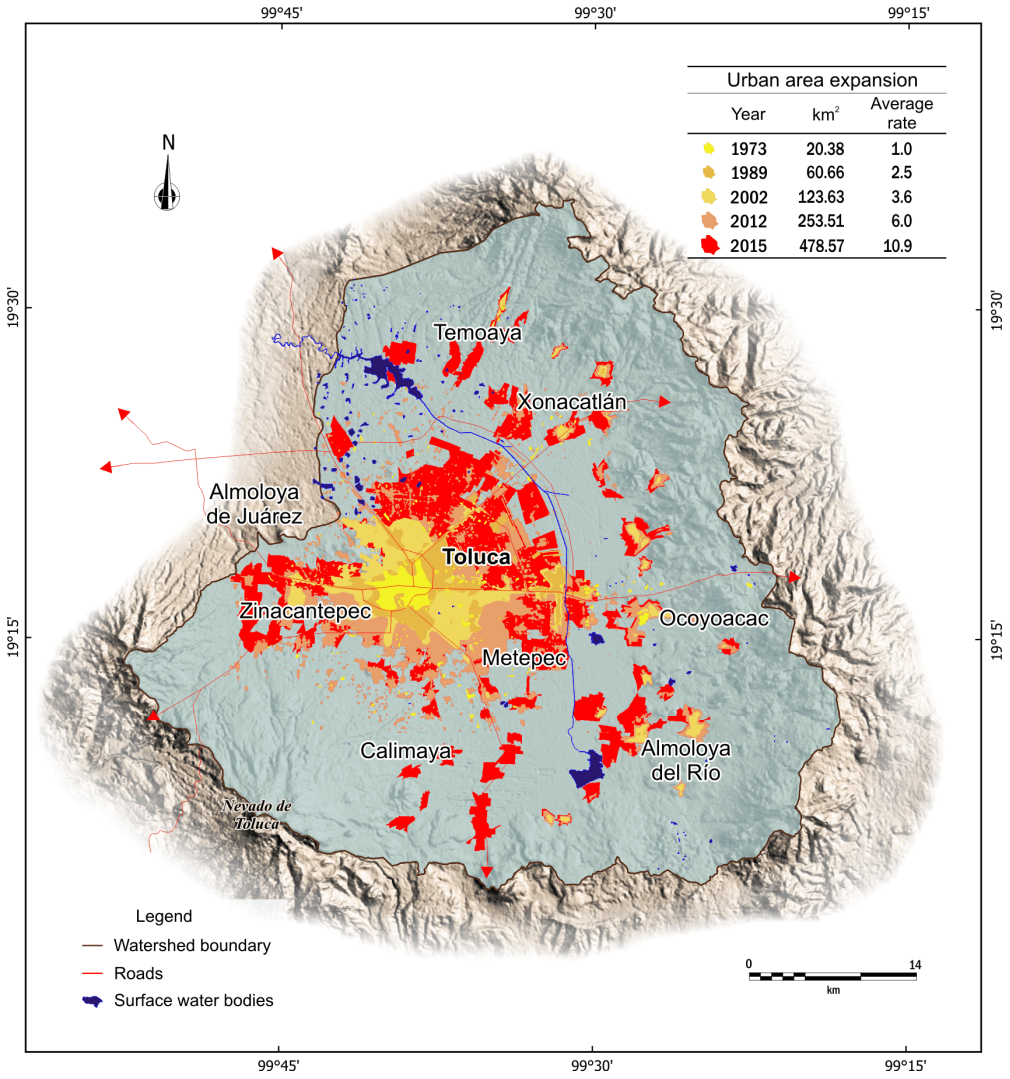

Figure 2. Map of the Toluca Basin showing a graphical comparison of the metropolitan urban area expansion in the Toluca Valley delimited using Landsat color-composite images from 1973 to 2015. The images are available from the USGS LandsatLook Viewer (https://landsatlook.usgs.gov/).

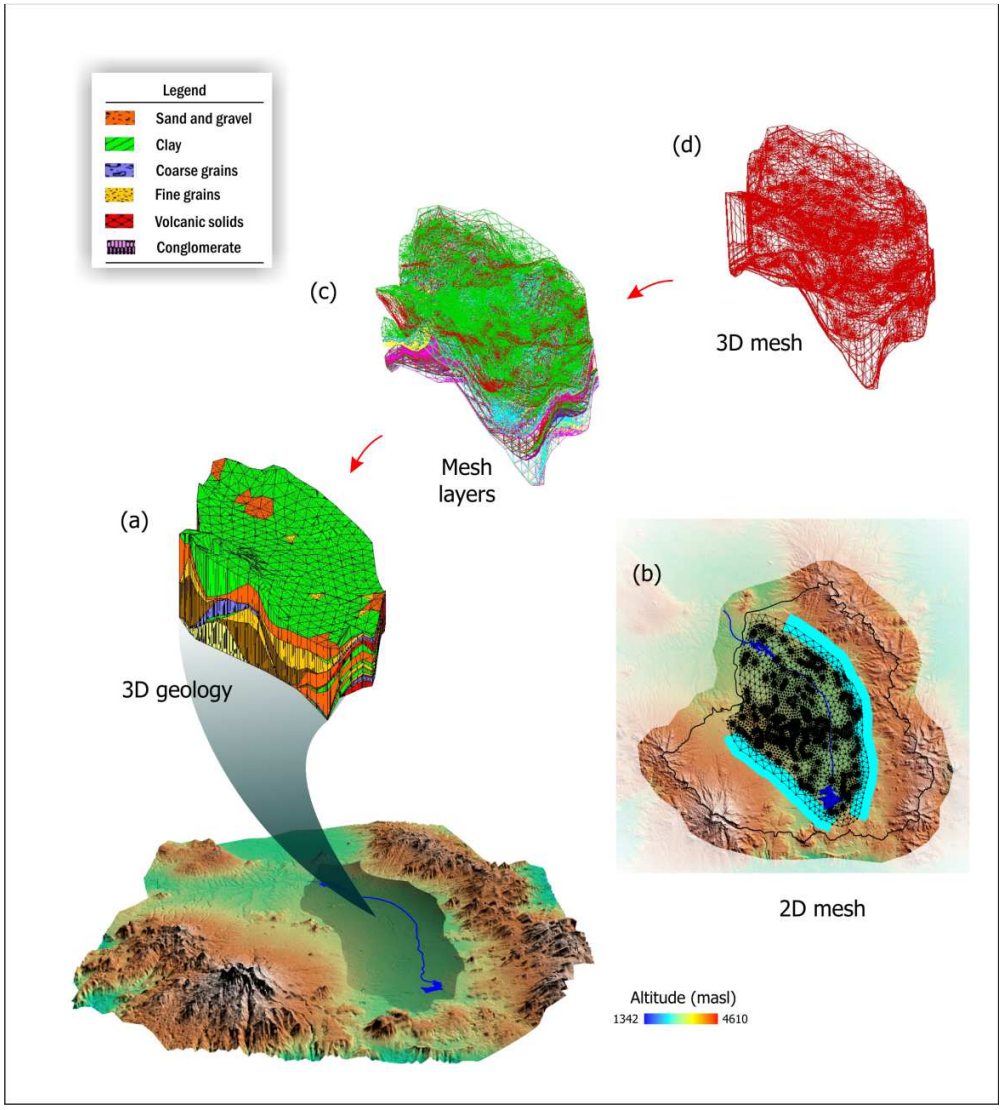

Figure 3. Processing chain for obtaining the 3D finite-element model domain. The 3D geology (a) is generated with the use of borehole logs and available cross sections, then using the 2D mesh (b) and the topography of the geologic layers, 15 topographically variable 2D layer meshes are extracted (c) and used to generate the 3D mesh (d). Location of the constant head boundary is also shown in (b) (modified from Calderhead et al. (2011)).

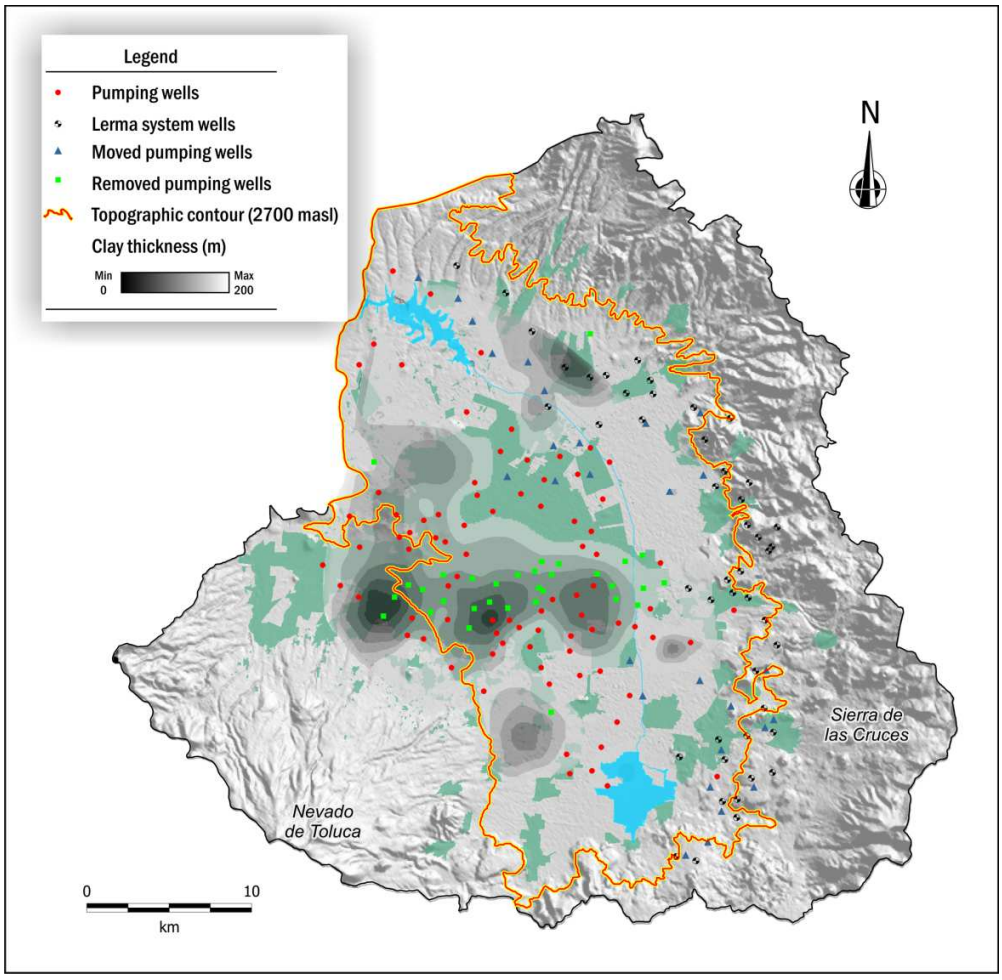

Figure 4. Distribution of simulated pumping wells for groundwater management scenarios for the Toluca aquifer system and spatial distribution of aggregate clay thickness (modified from Calderhead et al. (2012a)). Also shown is the metropolitan area for 2015 delimited using Landsat images.

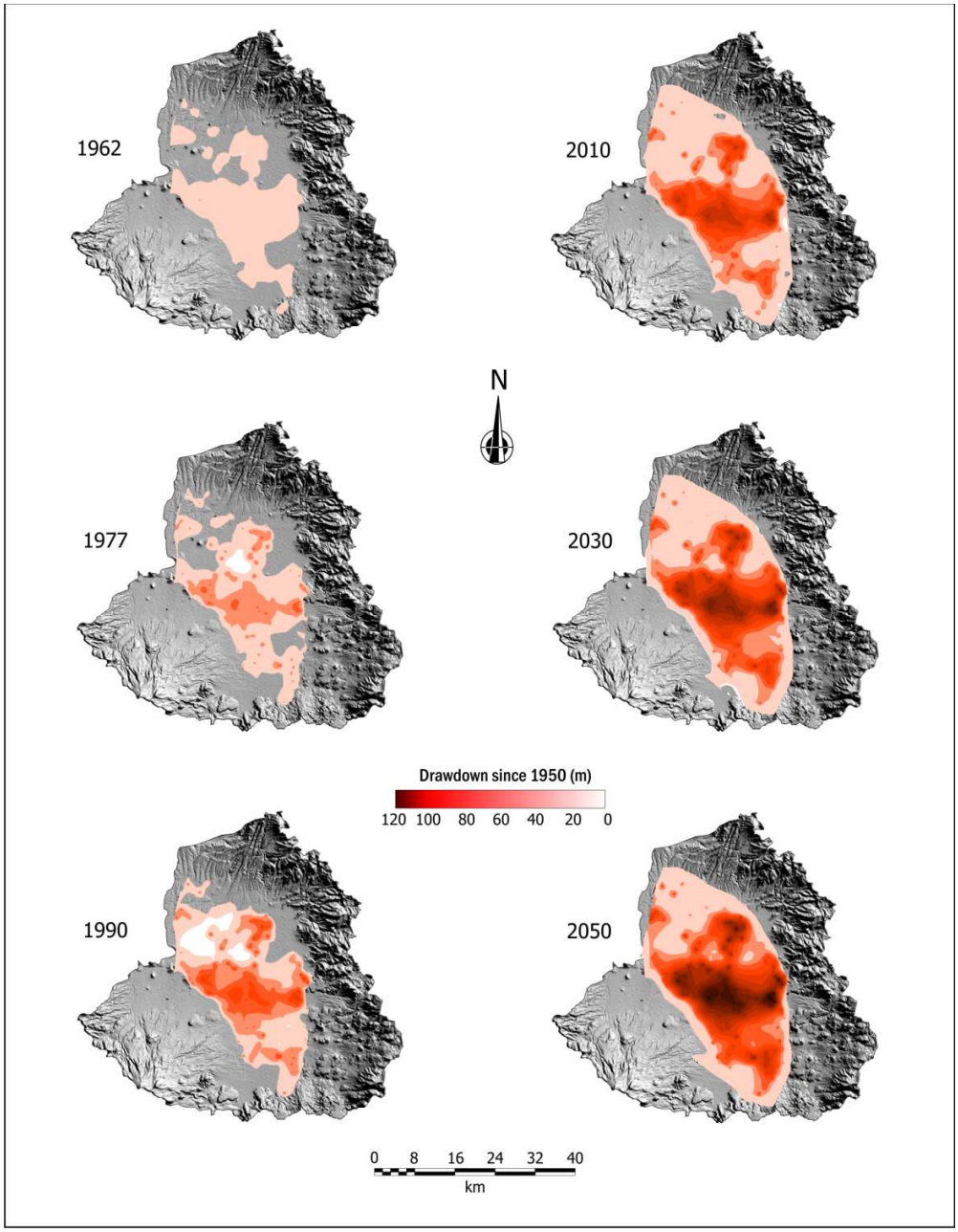

Figure 5. Evolution of regional drawdown in the Toluca Valley aquifer system from 1962 to 2050 simulated with HGS using 1950 levels as initial condition (scenario 3, modified from Calderhead et al. (2012b)).

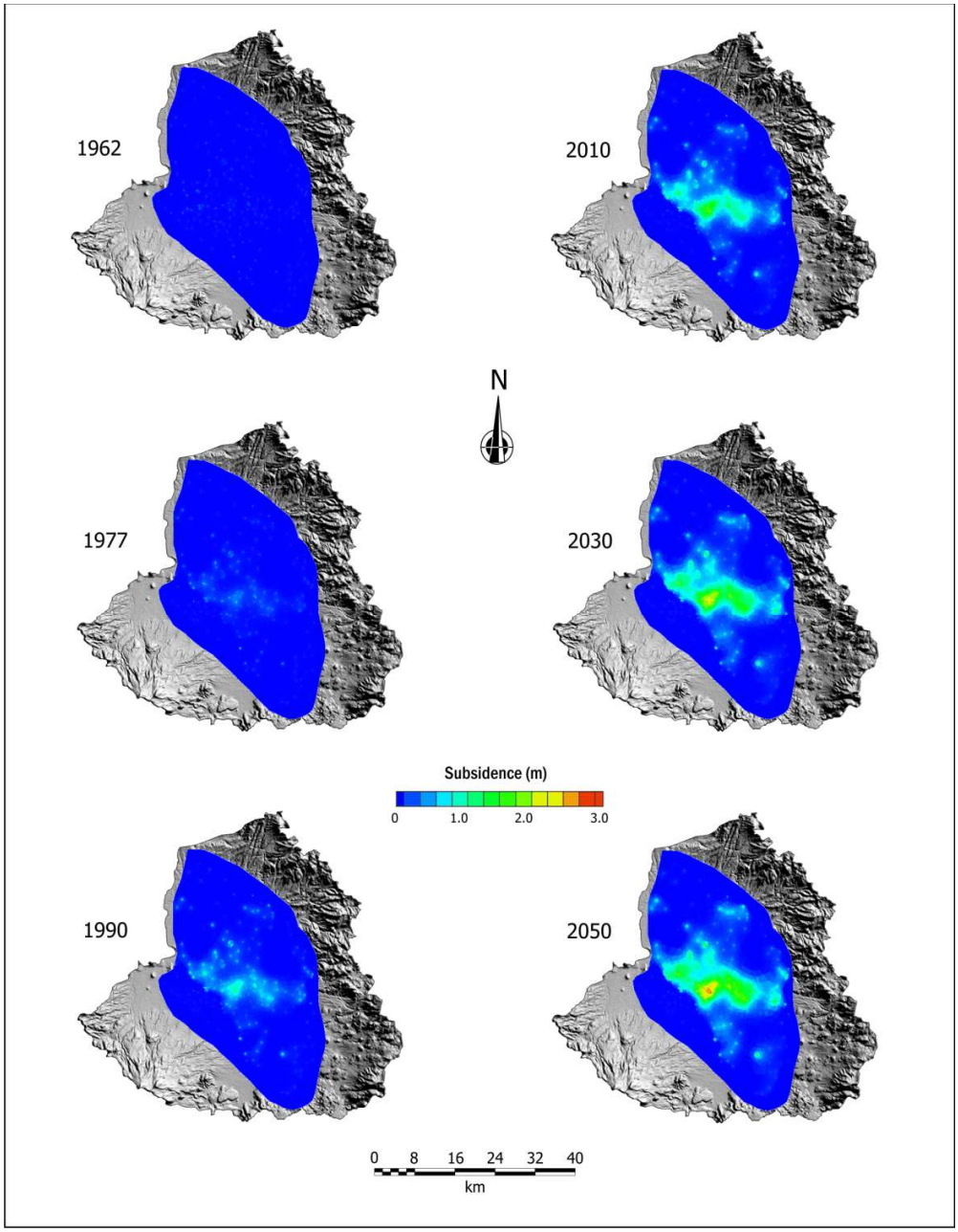

Figure 6. Evolution of regional land subsidence in the Toluca Valley aquifer system from 1962 to 2050 simulated with HGS (scenario 3, modified from Calderhead et al. (2012b)).

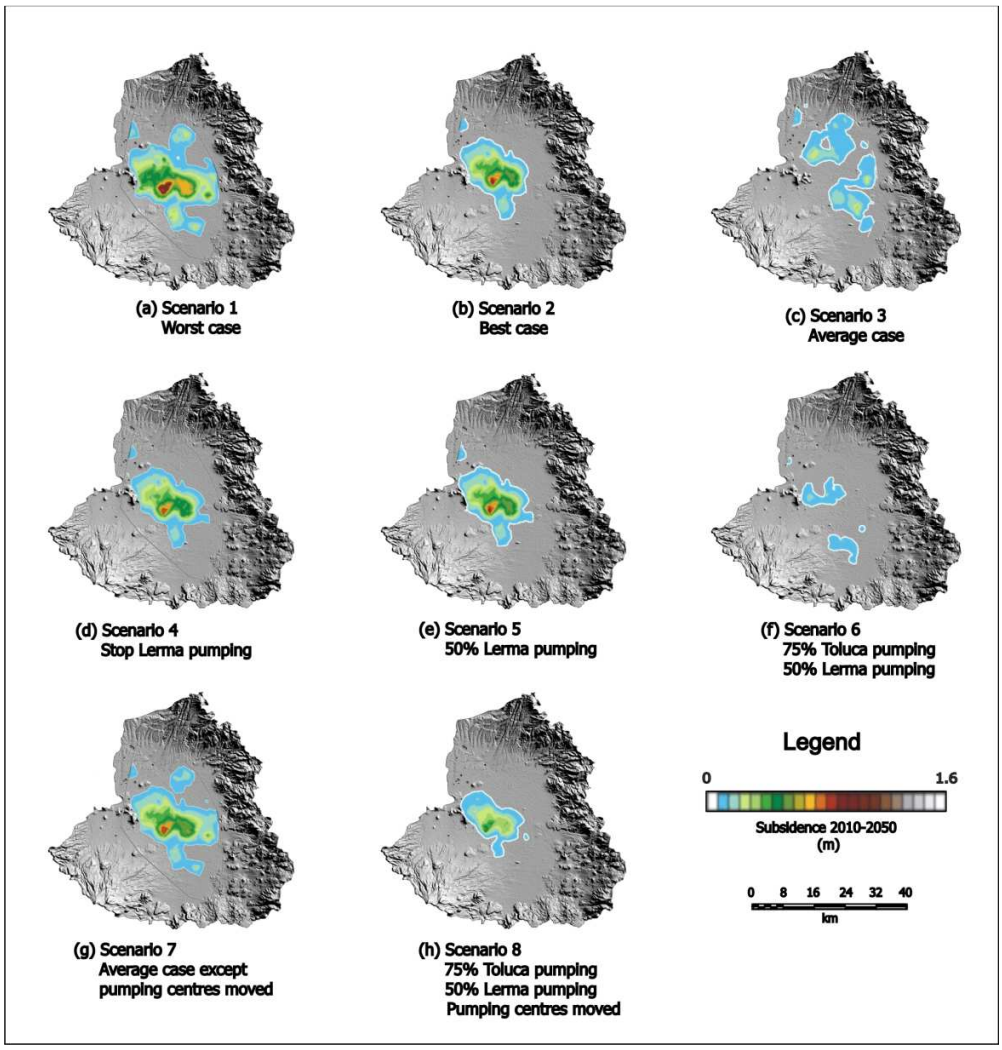

Figure 7. Simulation results for scenarios 1–8 showing total land subsidence simulated with HGS between 2010 and 2050 (scenario 3, modified from Calderhead et al. (2012b)).

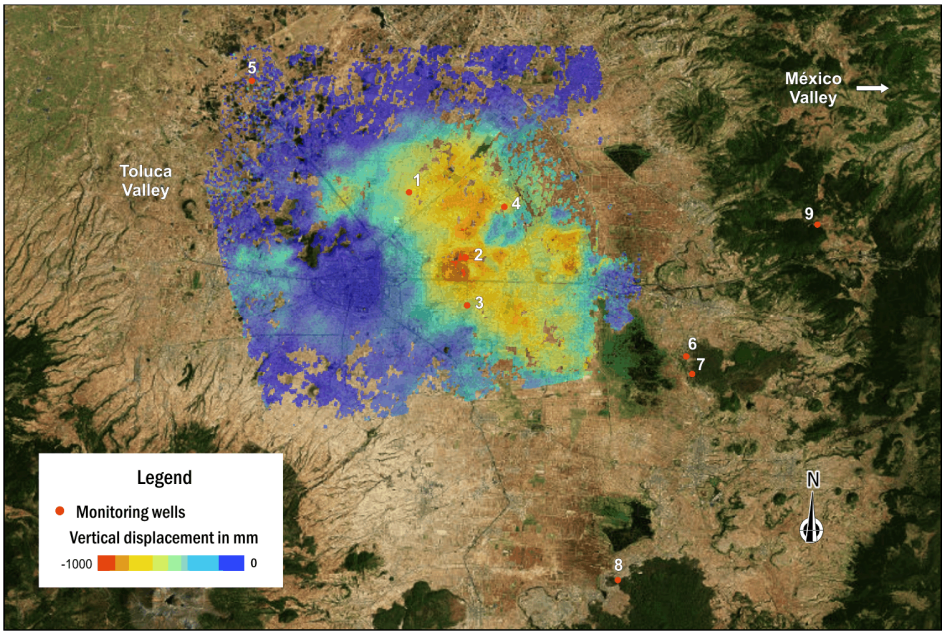

Figure 8. Total vertical subsidence for the period 2003–2016 produced by cumulating InSAR measurements from three SAR sensors. Some areas of the city have undergone 1 m of subsidence in 13 years. Temporal variation of the groundwater levels are shown in Figs. 9 and 10 for the monitoring wells 1–9.

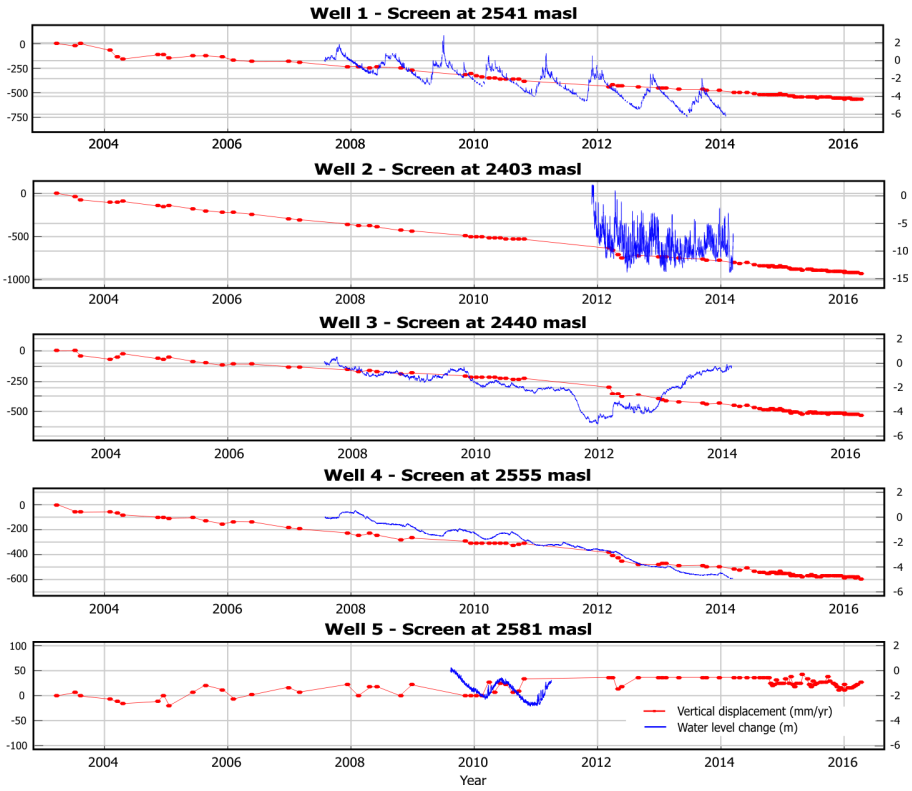

Figure 9. Groundwater level change in monitoring wells 1-5 and InSAR-derived vertical subsidence at their vicinity. For the general location of monitoring wells refer to Fig. 8.

Figure 10. Groundwater level change in monitoring wells 6–9. For the general location of monitoring wells refer to Fig. 8.

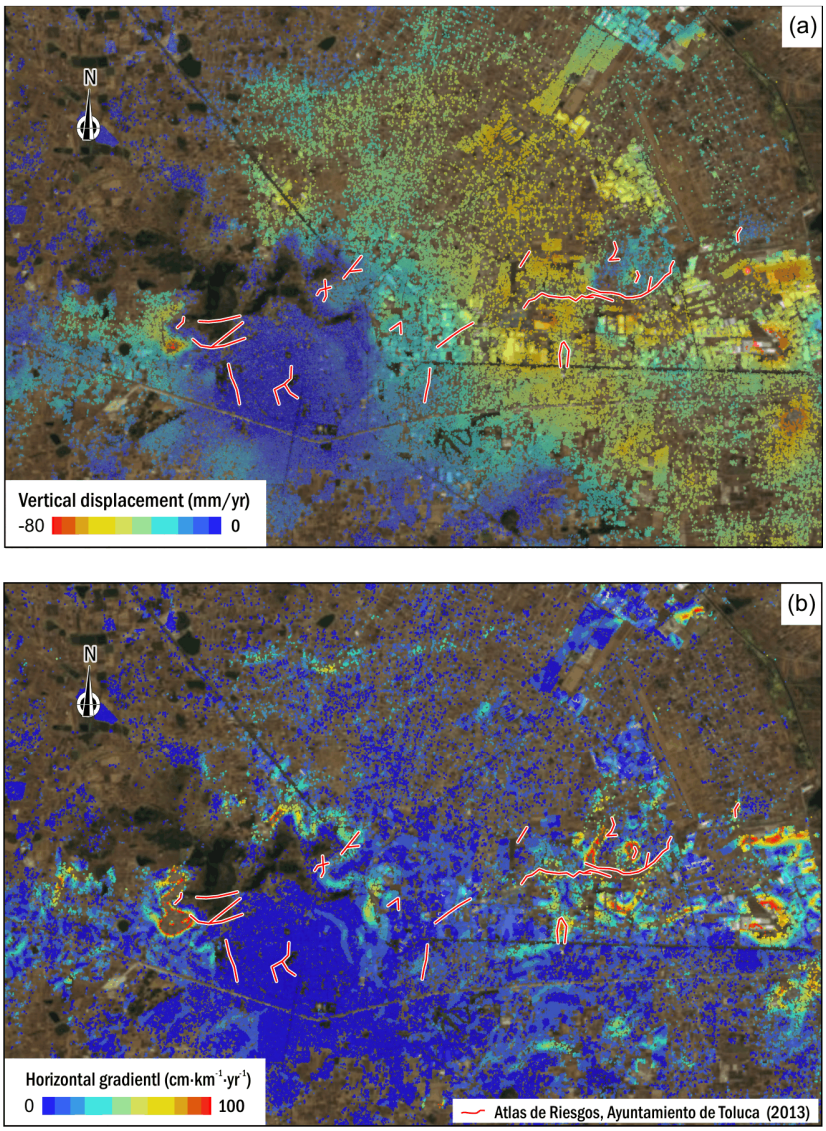

Figure 11. (a) Vertical displacement rates for the period 2014–2016 measured by processing 41 Sentinel-1A images using the PSI algorithm; (b) By solving the phase ambiguity individually for each ground target, PSI allows ground displacement measurements at the ground target resolution. Also shown is the latest ground fracturing map determined by the Ayuntamiento de Toluca (2013).

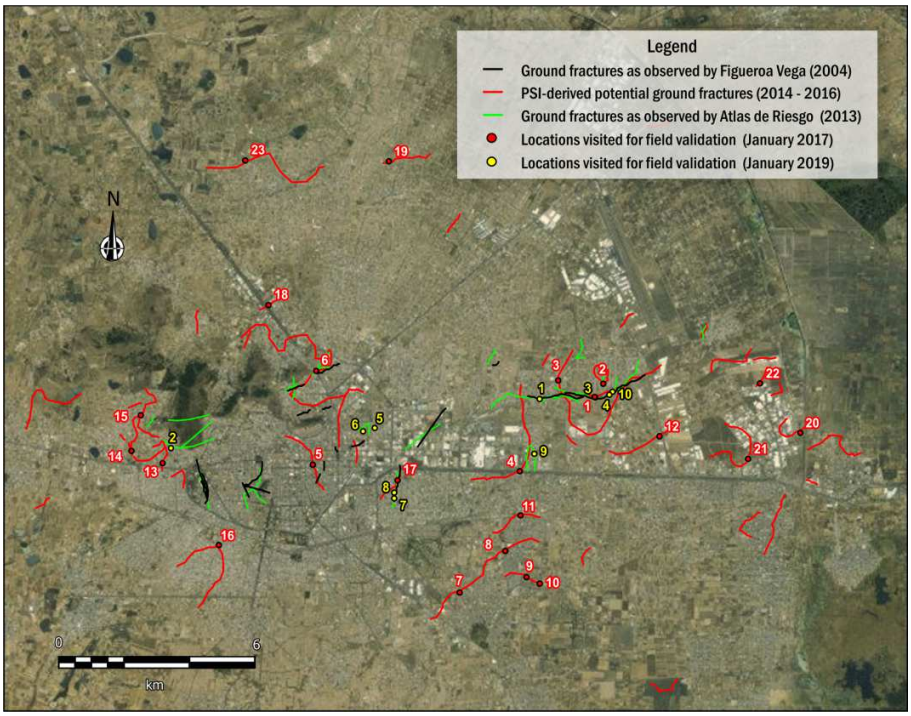

Figure 12. Comparison between potential surficial fractures manually drawn from the PSI-derived horizontal gradient map of vertical subsidence (Fig. 11) and the latest surficial fracture map from the Ayuntamiento de Toluca (2013) based on field observations.

Figure 13. Examples of ground fractures observed in the field while surveying the areas identified by PSI. The locations visited are all marked on Fig. 12.